Detailed analysis of the microwave-detected photoconductance decay in crystalline silicon

K. Lauer,[1,2,a)] A. Laades,[1] H. Übensee,[1] H. Metzner,[1,b)] and A. Lawerenz[1]
[1]*CiS Institut für Mikrosensorik GmbH, SolarZentrum Erfurt, Konrad-Zuse-Str. 14, 99099 Erfurt, Germany*
[2]*TU Ilmenau, Institut für Physik, Weimarer Str. 32, 98693 Ilmenau, Germany*

(Received 28 August 2008; accepted 7 October 2008; published online 19 November 2008)

An approach to evaluate the microwave-detected photoconductance decay (MWPCD) is developed, which allows to extract the minority carrier lifetime as a function of the excess carrier density from a single MWPCD measurement. The method is shown to be applicable to thin ($w \lesssim 200$ μm) silicon wafers with low minority carrier recombination at the surfaces and bulk lifetimes in the range of about 1–100 μs. Comparison of the MWPCD results with minority carrier lifetime measurements using the quasi-steady-state photoconductance method reveals very good agreement between both types of measurement. Only when the photoconductance exceeds 30% of the dark conductivity, is a deviation observed, because then the MWPCD signal is no longer directly proportional to the excess carrier density. Minority carrier trapping is found to affect the MWPCD signal only in the tail of the measured photoconductance decay. The evaluation method is used to map the interstitial iron content with high spatial resolution, as well as to determine the minority carrier trap density. An excellent agreement between numerical simulation and measured MWPCD signal is found revealing the assumptions made for the evaluation approach to be valid. This evaluation of the MWPCD measurement is well suited to characterize silicon of low purity and low crystalline quality, which is often employed to solar cells with high spatial resolution. © *2008 American Institute of Physics*.
[DOI: 10.1063/1.3021459]

I. INTRODUCTION

A widely used method to characterize the quality of crystalline silicon by means of the minority carrier recombination lifetime is the microwave-detected photoconductance decay (MWPCD)[1,2] measurement, which detects the decaying photoconductance after illumination. Much effort was spent on the interpretation of the measured MWPCD signal[3] in electronic grade silicon, which is used to fabricate semiconductor chips. Due to the rapidly growing photovoltaic industry, the demand for silicon for solar cells increases dramatically. In contrast with the extremely pure and hence expensive electronic grade silicon, the solar industry often employs silicon of low purity and low crystalline quality, which is still sufficient for comparatively high solar cell efficiencies.[4] This material, which includes multicrystalline silicon wafers originating from directional solidified ingots or from edge-defined film-fed growth as well as monocrystalline silicon wafers from very impure Czochralski ingots, is henceforth summarized under the term low-quality silicon. As discussed below in more detail, MWPCD measurements on low-quality silicon yield quite different signals as compared to measurements on electronic grade silicon and the interpretation of the former MWPCD measurements becomes difficult. A reasonable possibility to characterize low-quality silicon samples is to illuminate them with a constant bias light during the MWPCD measurement.[5–8] However, several MWPCD measurements at different bias light intensities are needed to obtain the minority carrier recombination lifetime.

We present a method to characterize low-quality silicon wafers by MWPCD measurements. An evaluation approach is applied to the measured MWPCD signal, which extracts the minority carrier lifetime as a function of the excess carrier density from a single photoconductance decay, and allows to gain additional information about the material. Section II shortly overviews the MWPCD method and introduces our evaluation approach. The main assumptions and limits of this approach are discussed. In Sec. III, the evaluation method is applied to measurements of the photoconductance decay and the results are compared with quasi-steady-state photoconductance (QSSPC) (Ref. 9) measurements. The evaluation method is demonstrated to reveal two additional pieces of information about the silicon quality in Sec. IV. First, a map of the interstitial iron content is determined based on the change in lifetime during the iron-boron pair defect reaction.[10] Second, the minority carrier trap density is obtained using the Hornbeck–Haynes[11] trapping model.

II. THEORY

A. Correlation between excess carrier density and microwave reflectivity

The generation of excess carriers in a silicon sample increases its conductivity and hence causes a change in the microwave reflectivity of the sample. This change in reflectivity can be measured by means of reflected microwaves.

a)Electronic mail: klauer@cismst.de.
b)Present address: FSU Jena, Institut für Festkörperphysik, Helmholtzweg 3, 07747 Jena, Germany.

 © 2008 American Institute of Physics

Downloaded 08 Oct 2013 to 221.130.18.182. This article is copyrighted as indicated in the abstract. Reuse of AIP content is subject to the terms at: http://jap.aip.org/about/rights_and_permissions

Kunst and Beck[1,2] developed the basics of this kind of measurement. They found, in the case of small perturbations, which means the excess conductivity $\Delta\sigma$ is much lower than the dark conductivity σ_0 ($\Delta\sigma \ll \sigma_0$), a relationship between the change in the reflected microwave power ΔP_r and the excess conductivity,[1]

$$\frac{\Delta P_r}{P_r(\sigma_0)} = \frac{1}{R(\sigma_0)}\left[\frac{\partial R(\sigma)}{\partial \sigma}\right]_{\sigma_0} \Delta\sigma = A(\sigma_0)\Delta\sigma, \tag{1}$$

where $P_r(\sigma_0)$ is the unperturbed reflected microwave power and $R(\sigma_0)$ is the reflectivity as a function of the dark conductivity. To obtain the sensitivity factor $A(\sigma_0)$, the reflectivity has to be calculated. This can be done using the dielectric multilayer model of Harbecke,[12] which was applied to microwave reflectivity of silicon.[13] Essentially this model is based on the transfer-matrix approach. If the sensitivity factor A is known for a specific sample and experimental setup, the absolute values of the excess conductivity and hence the excess carrier density Δn can be determined from the change in the reflectivity. The excess carrier density is related to the excess conductivity via

$$\Delta\sigma = q(\mu_n + \mu_p)\Delta n. \tag{2}$$

The electron and hole mobilities, μ_n and μ_p, respectively, are assumed to be independent of the excess carrier density; q denotes the elementary charge.

The above derivation applies only in the case of a homogeneous excess carrier profile in the region, which interacts with the microwaves. If the excess carriers are inhomogeneously distributed, the measured excess carrier density is an average of the local excess carrier density $\Delta n(\vec{x},t)$ over the measured volume V_m.[5] Therefore, the measured excess carrier density is referred to as $\Delta n_{\mathrm{av}}(t)$ from now on and is given by

$$\Delta n_{\mathrm{av}}(t) = \frac{1}{V_m}\int_{V_m} \Delta n(\vec{x},t)dV. \tag{3}$$

B. Determination of the bulk minority carrier lifetime

The determination of the bulk minority carrier lifetime by measuring the excess carrier decay is complicated by a recombination of excess carriers at the surfaces and by a strong dependence of the bulk lifetime on the excess carrier density. The first problem is solved experimentally, whereas the second one is treated by evaluating the complete excess carrier decay in the following.

The recombination processes in the silicon wafer can be split into recombination at the surface and recombination in the bulk. Both processes determine the measured effective minority carrier lifetime τ_{eff} and a distinction is difficult. The measured effective lifetime should be dominated by bulk recombination for a meaningful characterization of the silicon quality. To realize this condition, the most feasible method at present is a silicon nitride layer on the wafer surface,[14] which minimizes the surface recombination. Hence, the effective lifetime measured on wafers prepared in this way represents the bulk lifetime τ_b (Ref. 7), referred to as lifetime in the following.

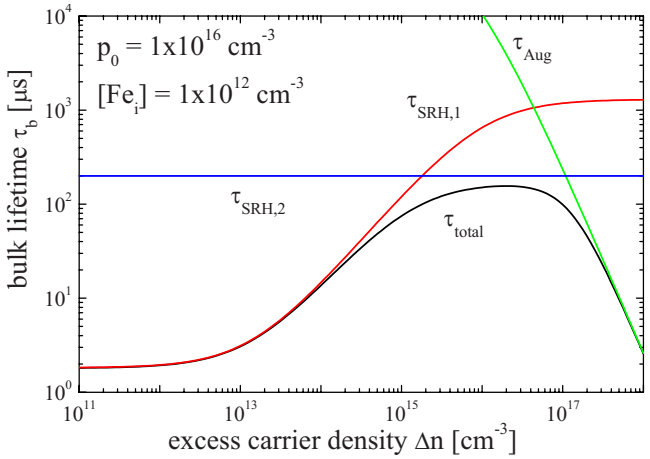

FIG. 1. (Color online) Bulk lifetime as a function of the excess carrier density in typical low-quality silicon.

Usually, the measured time decay of the excess carrier density is fitted by a single exponential function and the resulting time constant of the decay is interpreted as the lifetime. This simple interpretation of the measured excess carrier decay is valid only if the lifetime is independent of the excess carrier density. A comprehensive overview of lifetime measurements is given in Ref. 3.

However, the lifetime in low-quality silicon is frequently a strong function of the excess carrier density, due to a high density of different defects and the contamination with impurity atoms. Additionally, the lifetime may change under illumination due to various defect reactions. We will refer only to the lifetime that is stable during illumination in order to avoid errors caused by the averaging of several measurements. To illustrate the lifetime in a typical low-quality silicon wafer, we assumed realistic parameters and calculated the lifetime as a function of the excess carrier density. Figure 1 exemplifies the impact of three different recombination paths on the total lifetime τ_{total}. Two Shockley–Read–Hall (SRH) recombination centers[15] are assumed. The first one (SRH,1) accounts for the interstitial iron defect[16] and the second one (SRH,2) represents all other defects. Their lifetimes are denoted by $\tau_{\mathrm{SRH,1}}$ and $\tau_{\mathrm{SRH,2}}$, respectively. Additionally, Auger recombination[17] is implemented into the calculation using coefficients taken from Ref. 18. The total lifetime below an excess carrier density of $\Delta n = 10^{15}$ cm^{-3} is dominated by the first SRH lifetime as shown in Fig. 1. Above an excess carrier density of $\Delta n = 10^{17}$ cm^{-3} Auger recombination dominates the total lifetime and, in between, the second SRH lifetime has the main impact. The lifetime is found to be constant below the excess carrier density Δn_l (in this case $\Delta n_l = 10^{13}$ cm^{-3}), which characterizes the upper limit of the low injection region. So, the conventional evaluation of the measured excess carrier decay by means of a single exponential decay can only be applied if the initial excess carrier density of the decay is below this critical value Δn_l.

Downloaded 08 Oct 2013 to 221.130.18.182. This article is copyrighted as indicated in the abstract. Reuse of AIP content is subject to the terms at: http://jap.aip.org/about/rights_and_permissions

Unfortunately, lifetime measurements below Δn_l are not suitable to characterize low-quality silicon, which is used to produce solar cells, for various reasons. First, due to the low lifetime and the small excess carrier density compared to the equilibrium carrier density of usually $p_0 = 10^{16}$ cm^{-3}, the signal to noise ratio of the measurement is poor. Second, the excess carrier density of $\Delta n \approx 10^{14}$ cm^{-3} within a typical crystalline silicon solar cell under operating conditions at an illumination of 1 sun is one order of magnitude larger than Δn_l. So, the lifetime measured below Δn_l will not represent the carrier lifetime of a solar cell under working conditions. Finally, measurements of the excess carrier decay with Δn_l as initial excess carrier density are hampered by trapping[19] or trappinglike artifacts.[20] Hence, the extracted lifetime will not represent the actual recombination lifetime. These outlined problems to measure the lifetime by MWPCD even in regions with a strong dependence of the lifetime on the excess carrier density can be overcome as follows.

We propose a way to determine the lifetime as a function of the excess carrier density from a single MWPCD measurement. It simply relies on the increase in the initial excess carrier density and the measurement of the complete excess carrier decay. Subsequently, the logarithm of the excess carrier decay is differentiated with respect to time at every point of time numerically. This reveals the negative inverse lifetime and if the time is used as a parameter, the lifetime can be obtained as a function of the excess carrier density as well. To derive an equation, which gives the base for this evaluation method, the diffusion equation of the excess carriers has to be considered. The local density of the excess carriers in p-type silicon, $\Delta n(\vec{x},t)$, is achieved by solving the diffusion equation with proper initial and boundary conditions. For a vanishing electrical field the three dimensional diffusion equation is given by[21]

$$\frac{\partial \Delta n(\vec{x},t)}{\partial t} = G - U + D\left\{\frac{\partial^2 \Delta n(\vec{x},t)}{\partial x^2} + \frac{\partial^2 \Delta n(\vec{x},t)}{\partial y^2} + \frac{\partial^2 \Delta n(\vec{x},t)}{\partial z^2}\right\}, \tag{4}$$

where G and U are the generation and the recombination rates, respectively, and D denotes the diffusion coefficient. The bulk minority carrier lifetime τ_b is defined by

$$U(\Delta n) = \frac{\Delta n}{\tau_b(\Delta n)}. \tag{5}$$

If we assume a homogeneous carrier profile during the measurement, the diffusion term in Eq. (4) cancels out and the local excess carrier density equals the measured averaged excess carrier density. Without generation of carriers during the excess carrier decay we get, with some rearrangements, from Eqs. (4) and (5),

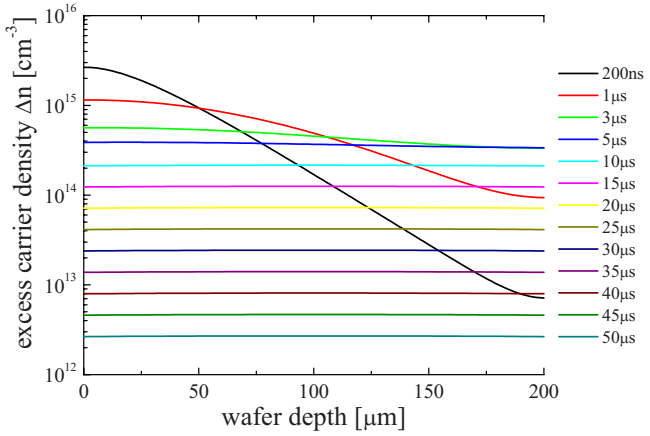

FIG. 2. (Color online) Excess carrier density as a function of wafer depth after laser excitation.

$$\tau_b(t) = -\left(\frac{d\{\ln[\Delta n_{\mathrm{av}}(t)]\}}{dt}\right)^{-1}. \tag{6}$$

Using this equation, the lifetime can be extracted as a function of the excess carrier density from the measured time decay of the excess carriers $\Delta n_{\mathrm{av}}(t)$.

C. Distribution of the excess carriers after laser excitation

The crucial assumption of a homogeneous excess carrier profile during the decay, which is made to develop the evaluation approach in Sec. II B, will be discussed in the following. The excess carrier distribution during the decay can be determined by solving the diffusion Eq. (4) with appropriate initial and boundary conditions. These conditions are given by the excitation of the carriers, the properties of the sample, and the experimental setup. We divided the problem into two parts. First, a laterally homogeneous excess carrier profile is assumed and the problem is simulated in the vertical dimension (z-direction) only. Second, we assumed a vertically homogeneous excess carrier profile in order to solve the diffusion equation in the lateral dimensions (x-y-plane).

The excess carrier density as a function of the wafer depth is simulated using the commercial ATLAS device simulator from Silvaco International, which solves the complete semiconductor equations. We assumed a 200 μm thick p-type ($p_0 = 10^{16}$ cm^{-3}) silicon sample with a surface recombination velocity at both surfaces of 100 cm/s. A constant bulk lifetime of 10 μs was chosen. Carriers are generated by a 200 ns laser pulse with a wavelength of 904 nm and an intensity of 16.4 W cm^{-2}. Figure 2 shows the results of the simulation. The excess carrier density is plotted as a function of the wafer depth after different time periods. Directly after turning off the laser (after 200 ns) the excess carrier density depends strongly on the wafer depth due to the exponential absorption law. However, after 3 μs, the excess carriers are already distributed nearly homogeneously over the whole wafer thickness. Hence, carrier diffusion in the z-direction can be neglected for the most part of the excess carrier decay and the local excess carrier density equals the averaged excess carrier density defined by Eq. (3) in this dimension.

Downloaded 08 Oct 2013 to 221.130.18.182. This article is copyrighted as indicated in the abstract. Reuse of AIP content is subject to the terms at: http://jap.aip.org/about/rights_and_permissions

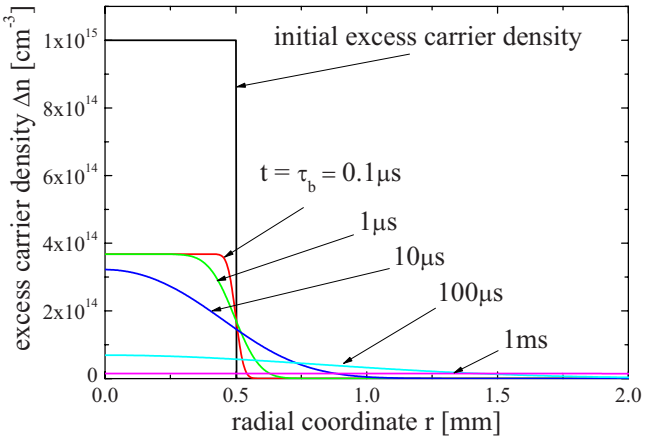

FIG. 3. (Color online) Excess carrier density as a function of the radial coordinate for different bulk lifetimes. The initial profile is plotted and also the profiles are shown, which form after exactly one bulk lifetime.

Nevertheless, the inhomogeneous excess carrier profile at the beginning of the decay affects the measurement, which will be discussed in Sec. III. The homogeneous carrier profile is limited to thin and surface passivated wafers. If the wafer becomes thicker, it takes longer until the excess carriers are homogeneously distributed and larger parts of the measured decay are perturbed. In the case of strong surface recombination, the excess carriers will not be distributed homogeneously at all.[22] In the vertical dimension, the bulk lifetime defines a lower limit for the applicability of our approach: if the bulk lifetime decreases, the fraction of the measureable decay, where the excess carriers are homogeneously distributed, decreases too. For a MWPCD signal, which ranges over about three orders of magnitude of the excess carrier density, the region, where the carriers are homogeneously distributed, is about 60% of the excess carrier decay if a 200 μm thick sample with a lifetime of 1 μs is investigated.

The experimental setup of a MWPCD device is usually optimized for high spatial resolutions and thus the spot size of the laser is small compared to the area, which reflects the microwaves. So, the radius of the excited area becomes close to the diffusion length of the carriers. To simulate the lateral diffusion of the excess carriers during the decay, we solved the diffusion Eq. (4) numerically using MATHEMATICA.[23] We transformed the diffusion equation into cylindrical coordinates and assumed a homogenous carrier profile in the z-direction. The radial symmetry of the experimental setup allows us to neglect derivatives with respect to the angular coordinate. Figure 3 shows the result of the numerical solutions. The excess carrier density is plotted versus the radial coordinate for different values of the lifetime, which is assumed to be independent of the excess carrier density. These curves are calculated for a time after the excitation, which equals the respective lifetime, in order to illustrate the smearing out of the sharp initial excess carrier density profile during the measurement. Usually, the smearing out has no effect on the measured averaged excess carrier density in silicon, which has a low and excess carrier independent lifetime,[24] because the measured area is much larger than the excited area. Only if the lifetime is very large and the excess carriers diffuse out of the measured area can the measured lifetime underestimate the actual one. Another problem occurs if the lifetime is not independent of the excess carrier density. In this case, the recombination of the excess carriers depends on the radial coordinate and the measured lifetime should be interpreted as a mean value. For our evaluation method, the smearing out leads to an overestimation of the actual excess carrier density and thus distorts the measurement. However we found by comparison with other measurement methods (see Sec. III C) and with numerical simulations (see Sec. IV C) that this effect has a minor impact on the results obtained by our experimental setup for carrier lifetimes below about 100 μs. Erroneous measurements due to the influence of lateral diffusion can be avoided if the laser spot size is chosen to be large compared to the diffusion length of the excess carriers.

The simulations in lateral and vertical dimensions confirm that a homogenous carrier profile during the excess carrier decay is a justifiable assumption. The requirements for the latter include: (i) thin ($w \lesssim 200$ μm) and (ii) surface passivated silicon wafers (iii) with a low bulk lifetime, which should be roughly in the region of $1\ \mu s < \tau_b < 100\ \mu s$. This lifetime range is typical for low-quality silicon.

III. EXPERIMENT

A. MWPCD measurements in low-quality silicon

The photoconductance decay is measured using a commercial MWPCD device (Semilab WT2000). A principle description of the experimental setup can be found in Refs. 1 and 2. Carriers are generated by a 200 ns laser pulse with a wavelength of 904 nm. The intensity of the laser is scalable up to 16.4 W cm^{-2}. For our measurements we use low-quality silicon wafers with a thickness below 200 μm and a surface passivation by silicon nitride.[14] If a high excitation density is chosen, the measured excess carrier decay, referred to as transient, is multiexponential as demonstrated in Fig. 4(a). Here, a multicrystalline silicon wafer with a boron doping density of $p_0 = 1.6 \times 10^{16}$ cm^{-3} is investigated. The measurements represent the average of 1024 transients after a laser excitation with different intensities. It is clearly visible that a linear fit to the exponentially scaled transients, as it is done in the conventional evaluation method, is inappropriate and leads to a loss of information about the material quality.

To avoid this loss of information, an approach to evaluate the measured excess carrier decay was developed in Sec. II B. This approach is applied to the data of Fig. 4(a). We use Eq. (6) to calculate the lifetime as a function of the MWPCD signal. The results are plotted in Fig. 4(b) for each laser intensity. Equation (6) includes a differentiation of the measured signal, which increases the noise. To reduce this effect, a moving average of the measured transient is calculated and Eq. (6) is subsequently applied. The applicability of this direct evaluation of the transient can be verified by comparing the measured transients with respective numerical simulations as demonstrated in Refs. 25 and 26 and Sec. IV C.

Downloaded 08 Oct 2013 to 221.130.18.182. This article is copyrighted as indicated in the abstract. Reuse of AIP content is subject to the terms at: http://jap.aip.org/about/rights_and_permissions

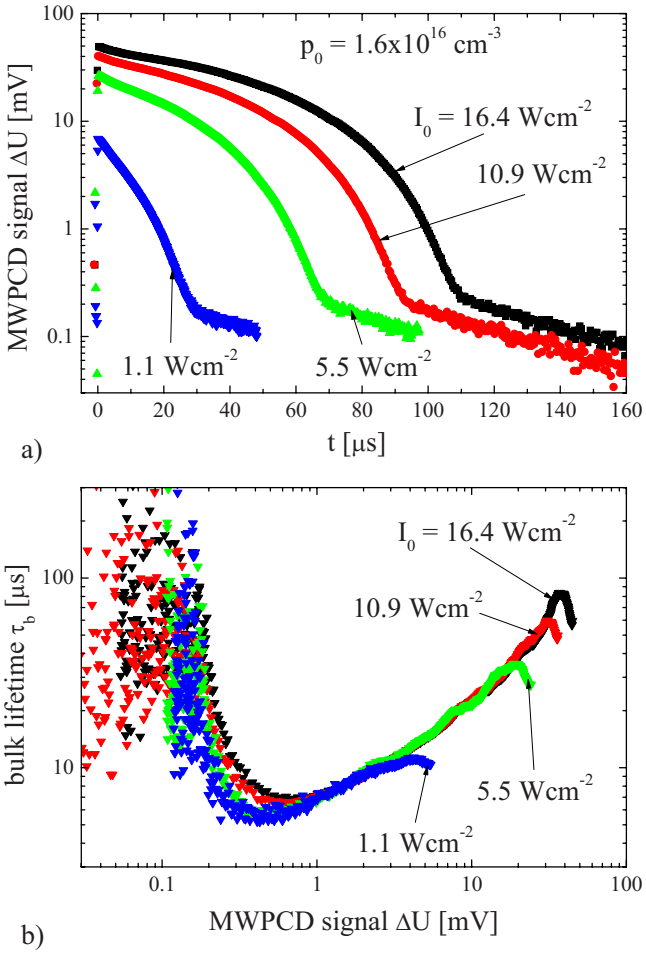

FIG. 4. (Color online) (a) The transients measured on a surface passivated multicrystalline silicon wafer with different intensities of the exciting laser are displayed. The average of 1024 transients is plotted respectively to reduce the noise of the signal. (b) The transients of part (a) are evaluated using Eq. (6).

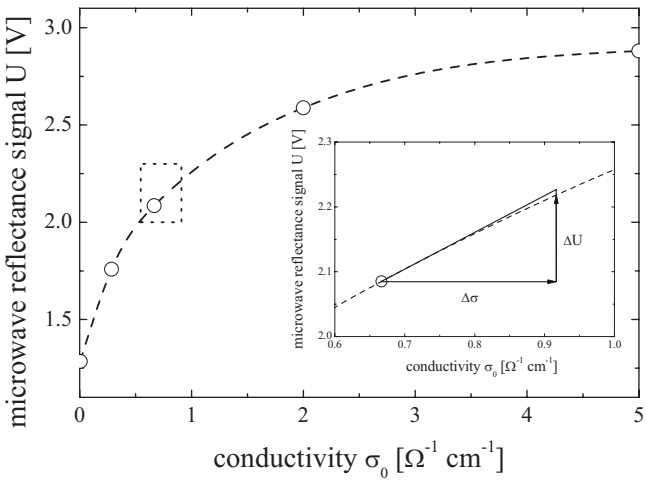

FIG. 5. The microwave reflectance signal at a frequency of $f=10.3$ GHz is measured for five differently doped float-zone silicon wafers with a thickness of $w=300$ μm. The dashed line is a spline interpolation. The impact of an increased conductivity due to laser excitation on the microwave reflection is exemplified at a conductivity within the typical range of the base doping of silicon solar cells.

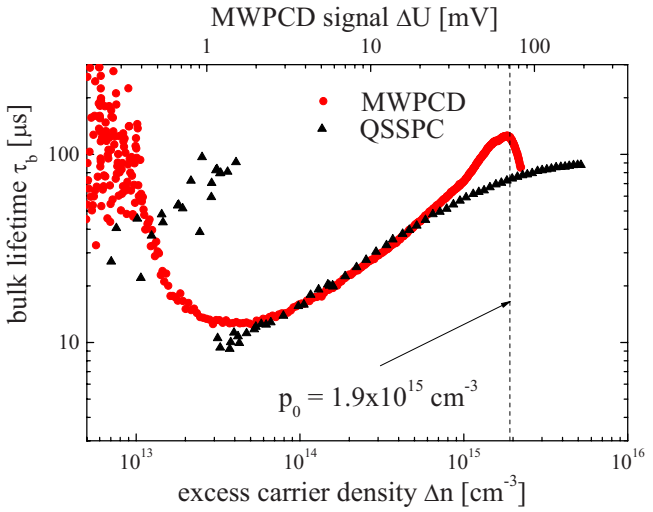

FIG. 6. (Color online) The bulk lifetime of a Czochralski silicon wafer is measured as a function of the excess carrier density with MWPCD and QSSPC. The comparison between both methods is used to calibrate the MWPCD signal.

B. Effect of nonlinear reflectance on MWPCD measurements

Since the reflectivity of silicon in the microwave range is not a linear function of the conductivity[1,13] the proportionality between the MWPCD signal and the excess conductivity has to be checked experimentally. Figure 5 shows microwave reflectance measurements of five differently doped float-zone silicon wafers with a thickness of $w=300$ μm. The frequency of the incident microwaves is $f=10.3$ GHz. The measurements are interpolated using cubic splines. A MWPCD measurement of a silicon wafer with a conductivity of $\sigma_0=0.67$ Ω^{-1} cm^{-1}, which is within the typical range of the solar cell base doping, is illustrated in the inset of Fig. 5. The excitation laser injects excess carriers with a density of about $\Delta n=4\times10^{15}$ cm^{-3} inducing an increased conductivity denoted by $\Delta\sigma$. This leads to an increased microwave reflectance signal ΔU, which is measured as a function of time after turning off the laser. Due to the nonlinearity of the microwave reflectance a slight deviation from the proportionality between excess conductivity and the change in the microwave reflection is observed. This deviation leads to a maximum error in the measurement of the lifetime of about 10%. This error decreases significantly during the photoconductance decay.

C. Calibration of the MWPCD signal

The MWPCD signal is only proportional to the excess carrier density as derived in Eq. (1). To obtain absolute values of the excess carrier density, the MWPCD signal has to be calibrated. This is done by comparing the MWPCD measurement with a QSSPC (Ref. 9) measurement, which determines the lifetime as a function of the excess carrier density, too. The QSSPC measurement method, which was developed by Sinton and Cuevas,[9] determines the photoconductance using an inductively coupled coil. The signal of this coil is calibrated using wafers with known resistivity. Now, if the bulk lifetime of a wafer is a function of the excess carrier

Downloaded 08 Oct 2013 to 221.130.18.182. This article is copyrighted as indicated in the abstract. Reuse of AIP content is subject to the terms at: http://jap.aip.org/about/rights_and_permissions

density, the MWPCD signal can be calibrated by a QSSPC measurement. The evaluated MWPCD signal is shifted until both lifetime curves coincide (see Fig. 6). This transformation determines the proportionality factor of Eq. (1) for this sample. The calibration routine has to be done only once for one type of wafer, because the proportionality factor depends mainly on the doping of the silicon. Using the calibration by a QSSPC measurement, a problem arises caused by the differing measurement spot sizes of the MWPCD (~ 1 mm^2) and QSSPC (~ 1 cm^2). If the lifetime varies laterally, as is it usually the case in multicrystalline silicon, the QSSPC and MWPCD measurements may differ quite strongly. Hence, in multicrystalline silicon a homogeneous region should be employed for calibration. To avoid this problem, a monocrystalline Czochralski silicon wafer was taken for the measurements and displayed in Fig. 6.

D. Interpretation of the MWPCD signal

Figures 6 and 4(b) can now be used to study the MWPCD measurement. The comparison of QSSPC and MWPCD lifetime measurements in Fig. 6 reveals a good agreement for the most part of the lifetime curve. The anomalous increase in the lifetime below an excess carrier density of $\Delta n = 2 \times 10^{13}$ cm^{-3} is caused by trapping effects.[19,20] These will be analyzed in Sec. IV C. The most part of the transient is found not to be affected by trapping artifacts. A slight increase in the lifetime compared to the QSSPC measurement before the rapid increase in the lifetime due to the trapping effects is observed in Fig. 6. This is caused by the impact of the lateral diffusion, which leads to an overestimation of the excess carrier density and hence to a higher measured lifetime. The doping density determined by a four-point probe measurement is additionally drawn into Fig. 6. By comparing the doping density with the MWPCD measurement, the region, in which the microwave signal is proportional to the excess carrier density, can be determined. We found that the excess conductivity can reach up to 30% of the dark conductivity ($\Delta\sigma < 0.3\sigma_0$) without losing proportionality. This is surprising because it is usually assumed that the excess conductivity has to be much smaller than the dark conductivity ($\Delta\sigma \ll \sigma_0$) (see Refs. 1 and 13 and references therein). Between the region where the signal is not proportional to the excess carrier density and the region affected by trapping, the measured lifetime represents the actual bulk lifetime.

Figure 4(b) demonstrates the impact of varying laser intensity on the lifetime measurement. The initial excess carrier density decreases but the lifetime curves lie on each other for the most part of the measurement. The slight decrease at the beginning of each measurement originates from the inhomogeneous carrier profile directly after turning off the laser as the signal of the reflected microwaves depends slightly on the distribution of the excess carriers in the wafer.[27] Hence, diverging from Eq. (3), the excess carriers near the front surface are stronger weighted in the measured signal than excess carriers at the rear. So, the diffusion of the carriers from the front to the rear will, even in absence of recombination, cause a decrease in the MWPCD signal.

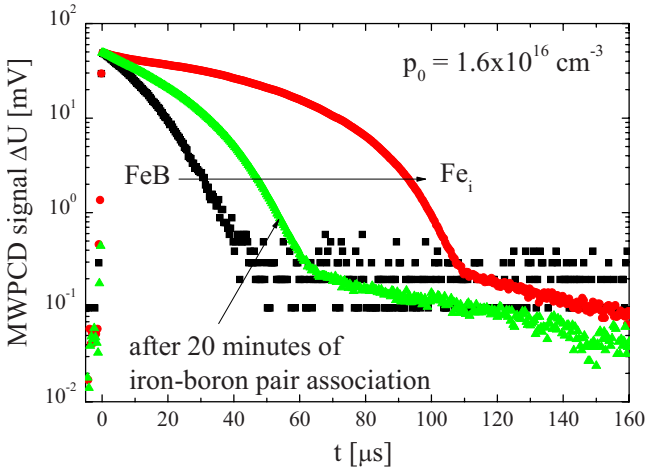

FIG. 7. (Color online) Transients measured in different states of the iron-boron pairs

IV. APPLICATION

The measurement of the lifetime as a function of the excess carrier density using the MWPCD provides the basis for advanced characterization methods using the MWPCD, such as interstitial iron mapping or minority carrier trap density determination.

A. Measurement of the interstitial iron content

Iron is one of the most common lifetime killing impurities in low-quality silicon.[28] In *p*-type silicon it forms metastable pairs with the boron acceptor.[29] The metastability of these pairs can be used to detect the concentration of interstitial iron. This was first applied to surface photovoltage (SPV) measurements[10] and later extended to QSSPC measurements.[30] As shown above, MWPCD measurements can be handled in the same way as QSSPC measurements. Hence, the interstitial iron detection method can also be applied to MWPCD measurements.

The effect of the iron-boron-pair dissociation on the MWPCD signal is demonstrated in Fig. 7, which shows the transients measured on a surface-passivated multicrystalline silicon wafer in different states of the iron-boron pairs. In the iron-boron-pair state only an average of four transients is taken in order to avoid considerable pair breaking during the measurement. The iron-boron pairs are dissociated using 10^5 pulses of the excitation laser. To split 100% of the iron-boron pairs and to reduce the noise of the signal an average of 1024 transients was taken in the interstitial-iron state.

If the transients in both states of the iron-boron pairs are evaluated by applying Eq. (6) [see Fig. 8(a)] and by using the QSSPC for calibration, the interstitial iron content [Fe$_i$] can be determined by inserting the lifetimes measured in both states into the following equation:[30]

$$[\mathrm{Fe}_i] = C(\Delta n)\left(\frac{1}{\tau_{\mathrm{Fe}_i}(\Delta n)} - \frac{1}{\tau_{\mathrm{FeB}}(\Delta n)}\right). \quad (7)$$

The prefactor $C(\Delta n)$ is calculated by applying the SRH theory with the parameters of the iron-boron-pair state[31] and the interstitial-iron state.[16] The lifetime in the latter states is

Downloaded 08 Oct 2013 to 221.130.18.182. This article is copyrighted as indicated in the abstract. Reuse of AIP content is subject to the terms at: http://jap.aip.org/about/rights_and_permissions

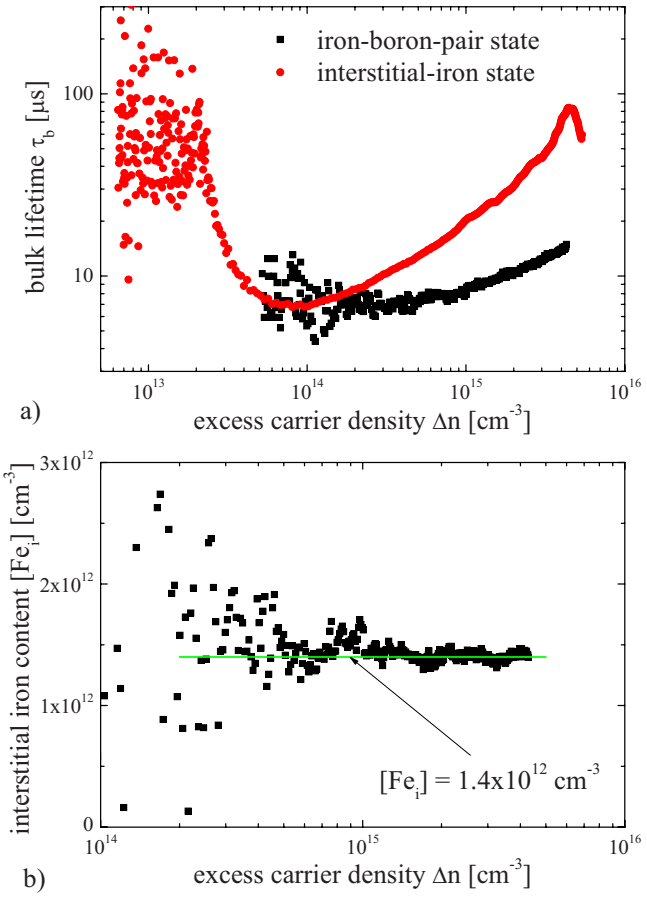

FIG. 8. (Color online) (a) The transients of Fig. 7 are evaluated using Eq. (6). Calibration was done by comparison with a QSSPC measurement. (b) The interstitial iron content is calculated as a function of the excess carrier density from the evaluated transients of part (a).

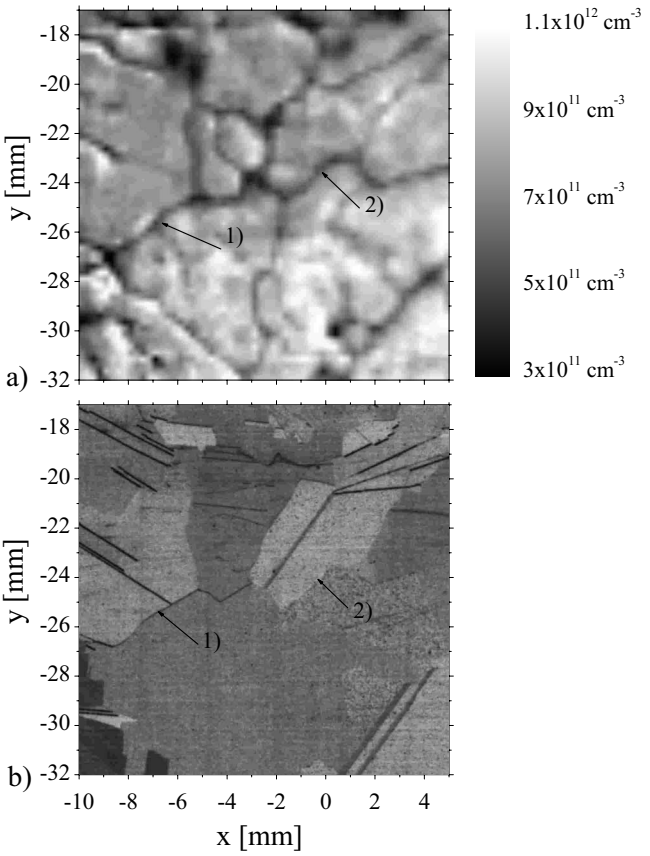

FIG. 9. The interstitial iron map (a) of a multicrystalline silicon wafer is compared with a scan image (b) with inverted brightness.

denoted by τ_{FeB} and τ_{Fe_i}, respectively. Figure 8(b) shows the interstitial iron content as a function of the excess carrier density calculated by Eq. (7) from the MWPCD measurements displayed in Fig. 8(a). To take into account the dissociation of the iron-boron pairs by laser excitation in the iron-boron-pair state, we assumed that 10% of the iron-boron pairs are dissociated during the first measurement. The interstitial iron content does, of course, not depend on the excess carrier density. Nevertheless, this plot can be used to study the accuracy of the measurement method itself. The constancy of the interstitial iron content for the most part of the measurement as shown in Fig. 8(b) confirms our approach to be accurate. Only for low excess carrier densities, the noise of the signal in the iron-boron-pair state disturbs the result of the interstitial iron content.

B. Mapping of the interstitial iron content

Interstitial iron is often distributed inhomogeneously due to the inhomogeneities of the material or due to diffusion processes in low-quality silicon wafers. Therefore, spatially resolved mappings of the interstitial iron content are of great interest. For this purpose several methods such as SPV mapping,[10] infrared lifetime mapping,[32] photoluminescence mapping,[33] and MWPCD mapping (conventional evaluation method)[34] are used. The latter three methods are restricted due to difficulties related to the exact local excess carrier density at which the measurements are done.[33] To overcome these problems, we evaluate the transients at every point of the wafer and subsequently calculate the interstitial iron content at a constant excess carrier density. An interstitial iron map derived by this method is displayed in Fig. 9(a). If the interstitial iron map is compared with the scan image of the wafer in Fig. 9(b), a reduced interstitial iron content at the grain boundaries is clearly visible (see arrows 1 and 2).

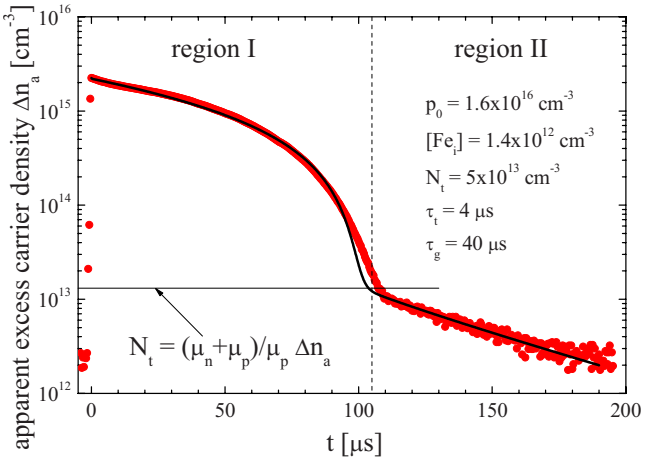

FIG. 10. (Color online) Measured and simulated transients are compared. The way to determine the trap density is demonstrated.

Downloaded 08 Oct 2013 to 221.130.18.182. This article is copyrighted as indicated in the abstract. Reuse of AIP content is subject to the terms at: http://jap.aip.org/about/rights_and_permissions

C. Determination of the minority carrier trap density

As we have already observed in Figs. 4(a) and 7, the transient of low-quality silicon reveals two regions, typically. In region I the lifetime shows a strong variation with excess carrier density. Region II, which occurs for low excess carrier densities, is dominated by a monoexponential decay. A specific example for this phenomenon is shown in Fig. 10. For the sample investigated in Fig. 10, the transient below about 100 μs is multiexponential due to the SRH dominated lifetime (see Fig. 1). Above 100 μs the transient becomes monoexponential revealing an anomalous high lifetime for low excess carrier densities as shown in Fig. 4(b). This region II can be used for a further evaluation of the material quality.

There are two physical reasons discussed in the literature that explain those transients at low excess carrier densities. The first explanation assumes a state within the band gap, which only interacts with one band. This situation is described by the Hornbeck–Haynes[11] trapping model and will be applied below. The second explanation of an increased lifetime at low excess carrier densities is given by the depletion region modulation effect.[20,35] For silicon nitride passivated low-quality silicon wafers the latter effect can be neglected.[36]

Applying the Hornbeck–Haynes[11] trapping model to the measured transient, the density of the trap states N_t can be determined. The excess carrier density $\Delta n(t)$ and the density of carriers within the trap n_t are given by a differential equation system

$$\frac{d\Delta n}{dt} = G - \frac{\Delta n}{\tau_b(\Delta n)} + \frac{n_t}{\tau_g} - \frac{\Delta n(1 - n_t/N_t)}{\tau_t}, \tag{8}$$

$$\frac{dn_t}{dt} = -\frac{n_t}{\tau_g} + \frac{\Delta n(1 - n_t/N_t)}{\tau_t}. \tag{9}$$

Here, G and $\tau_b(\Delta n)$ are the generation and the lifetime due to SRH recombination, respectively. The trap specific parameters are the trap density N_t, the mean time an electron spends in the trap τ_g, and the mean time an electron spends in the conduction band if all traps are empty τ_t. Measurements of the excess conductance reveal an apparent excess carrier density Δn_a, which takes into account the actual excess carrier density and a carrier density term caused by the trapped carriers[11]

$$\Delta n_a = \Delta n + \frac{\mu_p}{\mu_p + \mu_n} n_t. \tag{10}$$

The complete differential equation system of Eqs. (8) and (9) has to be solved to approximate transient measurements. Nevertheless, the trap density can be extracted from the transient in a simplified manner. In region I of Fig. 10 it is assumed that all traps are filled ($n_t = N_t$) and that the excess carrier density is larger than the carrier density within the traps ($\Delta n \gg n_t$). Hence the measured apparent excess carrier density in Eq. (10) equals the excess carrier density $\Delta n_a = \Delta n$. This changes in region II. There the excess carrier density becomes smaller than the carrier density within the traps ($\Delta n \ll n_t$) caused by specific parameters of the traps.[19] A small trap escape ratio τ_t/τ_g of the order of 0.1–0.01 in combination with a small recombination lifetime τ_b causes the carriers to recombine immediately after they are released from the trap into the conduction band. Hence, region II of the measured excess carrier density is dominated by the carrier density within the traps and Eq. (10) becomes $\Delta n_a = [\mu_p/(\mu_p + \mu_n)] n_t$. Thus the measured excess carrier density at the kink $\Delta n_{a,\mathrm{kink}}$ of the transient (transition from region I to region II) represents the trap density N_t as indicated in Fig. 10. This result is further confirmed by our model calculations, which are described in the following.

For comparison of the measured MWPCD signal with the theoretical predictions we solved the differential equation system Eqs. (8) and (9) numerically using MATHEMATICA.[23] The bulk lifetime $\tau_b(\Delta n)$ is taken from the model derived in Sec. II B using the specific parameters of this sample for the doping density ($p_0 = 1.6 \times 10^{16}$ cm^{-3}) and the interstitial iron content ($[\mathrm{Fe}_i] = 1.4 \times 10^{12}$ cm^{-3}). Four parameters, which are the initial excess carrier density Δn_0, the trap density N_t, and the trap time constants τ_t and τ_g, are adjusted to achieve the best approximation of the measurement. The results of the simulation are displayed in Fig. 10. A very good agreement between measurement and simulation is found, which reveals the lifetime model and the Hornbeck–Haynes trapping model to be appropriate in describing the measured excess carrier decay. The impact of the lateral diffusion as discussed in Sec. II C is observed as a slight deviation between simulation and measurement before the kink in the transient.

V. CONCLUSION

The MWPCD measurement is a well-known method to characterize the quality of crystalline silicon. Nevertheless, in the case of silicon of low purity and low crystalline quality, which is often employed for solar cells and is referred to as low-quality silicon, the interpretation of the MWPCD signal has to be adapted and thus can be used to gain more information about silicon quality. The MWPCD is investigated in detail in order to characterize low-quality silicon wafers. An evaluation method of the MWPCD signal is developed, which allows an extraction of the minority carrier lifetime as a function of the excess carrier density from a single MWPCD measurement. It is applicable for thin ($w \lesssim 200$ μm) and surface passivated silicon wafers, which have a lifetime in the region of about 1–100 μs. The results of our approach are compared to QSSPC measurements revealing a very good agreement for most parts of the MWPCD lifetime curve. The deviations between both signals are explained by the effect of the lateral and vertical carrier diffusion during the MWPCD measurement. The proportionality between MWPCD signal and excess carrier density is determined to be valid up to 30% of the dark conductivity. Minority carrier trapping is found to have an impact only at the tail of the photoconductance decay. By applying the new evaluation approach, two additional quality parameters of the material can be measured with the MWPCD tool: (i) a two-dimensional map of the interstitial iron content is measured to investigate especially multicrystalline silicon and (ii) the Hornbeck–Haynes trapping model is applied to determine

Downloaded 08 Oct 2013 to 221.130.18.182. This article is copyrighted as indicated in the abstract. Reuse of AIP content is subject to the terms at: http://jap.aip.org/about/rights_and_permissions

the minority carrier trap density. An excellent agreement between numerical simulations and measured MWPCD signal confirms the assumptions made for the evaluation method to be valid.

ACKNOWLEDGMENTS

The authors thank M. Blech for critical reading of the manuscript. One of the authors (K.L.) thanks G. Gobsch for his continuous support. The funding of this work by the State of Thuringia under Project DEFIS (Grant No. 2006 WF 0100) is gratefully acknowledged.

[1]M. Kunst and G. Beck, J. Appl. Phys. **60**, 3558 (1986).
[2]M. Kunst and G. Beck, J. Appl. Phys. **63**, 1093 (1988).
[3]D. C. Gupta, W. M. Hughes, and F. R. Bacher, ASTM Report No. STP1340, 1998.
[4]Several solar cell manufacturers use electronic grade silicon to produce high efficiency solar cells.
[5]P. A. Basore and B. R. Hansen, in Proceedings of the 21st IEEE Photovoltaics Specialists Conference (IEEE, New York, 1990), p. 374.
[6]R. Brendel, Appl. Phys. A: Mater. Sci. Process. **60**, 523 (1995).
[7]J. Schmidt and A. G. Aberle, J. Appl. Phys. **81**, 6186 (1997).
[8]J. Schmidt, IEEE Trans. Electron Devices **46**, 2018 (1999).
[9]R. Sinton and A. Cuevas, Appl. Phys. Lett. **69**, 2510 (1996).
[10]G. Zoth and W. Bergholz, J. Appl. Phys. **67**, 6764 (1990).
[11]J. Hornbeck and J. Haynes, Phys. Rev. **97**, 311 (1955).
[12]B. Harbecke, Appl. Phys. B: Lasers Opt. **39**, 165 (1986).
[13]M. Schöfthaler and R. Brendel, J. Appl. Phys. **77**, 3162 (1995).
[14]T. Lauinger, J. Schmidt, A. G. Aberle, and R. Hezel, Appl. Phys. Lett. **68**, 1232 (1996).
[15]W. Shockley and W. Read, Phys. Rev. **87**, 835 (1952).
[16]A. A. Istratov, H. Hieslmair, and E. R. Weber, Appl. Phys. A: Mater. Sci. Process. **69**, 13 (1999).
[17]A. R. Beatti and P. T. Landsberg, Proc. R. Soc. London, Ser. A **429**, 16 (1958).
[18]J. Dziewior and W. Schmid, Appl. Phys. Lett. **31**, 346 (1977).
[19]D. Macdonald and A. Cuevas, Appl. Phys. Lett. **74**, 1710 (1999).
[20]D. H. Neuhaus, P. J. Cousins, and A. G. Aberle, in Proceedings of the Third World Conference on Photovoltaic Energy Conversion (IEEE, New York, 2003).
[21]S. M. Sze, *Physics of Semiconductor Devices*, 2nd ed. (Wiley, New York, 1981).
[22]Y. Ogita, J. Appl. Phys. **79**, 6954 (1996).
[23]I. Wolfram Research, *Mathematica Edition: Version 6* (Wolfram Research, Inc., Champaign, 2007).
[24]M. Y. Ghannam, S. F. Mahmoud, and J. F. Nijs, J. Appl. Phys. **81**, 2665 (1997).
[25]R. K. Ahrenkiel, B. M. Keyes, and S. Johnston, Surf. Eng. **16**, 54 (2000).
[26]K. Lauer, A. Laades, H. Uebensee, and A. Lawerenz, Mater. Sci. Eng., B (in press).
[27]F. P. Giles, R. J. Schwartz, and J. L. Gray, in Proceedings of the 23rd IEEE Photovoltaics Specialists Conference (IEEE, New York, 1993), p. 299.
[28]A. Istratov, T. Buonassisi, R. McDonald, A. Smith, R. Schindler, J. Rand, J. Kalejs, and E. R. Weber, J. Appl. Phys. **94**, 6552 (2003).
[29]K. Graff and H. Pieper, J. Electrochem. Soc. **128**, 669 (1981).
[30]D. Macdonald, L. Geerligs, and A. Azzizi, J. Appl. Phys. **95**, 1021 (2004).
[31]D. Macdonald, A. Cuevas, and J. Wong-Leung, J. Appl. Phys. **89**, 7932 (2001).
[32]J. Henze, P. Pohl, C. Schmiga, M. Dhamrin, T. Saitoh, I. Yamaga, and J. Schmidt, in Proceedings of the 20th European Photovoltaic Solar Energy Conference (WIP, Munich, 2005), p. 769.
[33]D. Macdonald, J. Tan, and T. Trupke, J. Appl. Phys. **103**, 073710 (2008).
[34]C. Swiatkowski, in *Recombination Lifetime Measurements in Silicon*, edited by D. C. Gupta, W. M. Hughes, and F. R. Bacher (ASTM, West Conshohocken, 1998), p. 80.
[35]P. J. Cousins, D. H. Neuhaus, and J. E. Cotter, J. Appl. Phys. **95**, 1854 (2004).
[36]M. C. Schubert, S. Riepe, S. Bermejo, and W. Warta, J. Appl. Phys. **99**, 114908 (2006).

Downloaded 08 Oct 2013 to 221.130.18.182. This article is copyrighted as indicated in the abstract. Reuse of AIP content is subject to the terms at: http://jap.aip.org/about/rights_and_permissions